Aging Cell (2012) **11,** pp1017–1026 Doi: 10.1111/acel.12002

Diabetes exacerbates amyloid and neurovascular pathology in aging-accelerated mice

Antonio Currais,[1] Marguerite Prior,[1] David Lo,[2] Corinne Jolivalt,[3] David Schubert[1] and Pamela Maher[1]

[1]The Salk Institute for Biological Studies, Laboratory of Cellular Neurobiology, 10010 N. Torrey Pines Rd, La Jolla, CA 92037, USA
[2]The Salk Institute for Biological Studies, Laboratory of Neuronal Structure and Function, 10010 N. Torrey Pines Rd, La Jolla, CA 92037, USA
[3]University of California San Diego, Department of Pathology, 9500 Gilman Dr., La Jolla, CA 92093, USA

Summary

Mounting evidence supports a link between diabetes, cognitive dysfunction, and aging. However, the physiological mechanisms by which diabetes impacts brain function and cognition are not fully understood. To determine how diabetes contributes to cognitive dysfunction and age-associated pathology, we used streptozotocin to induce type 1 diabetes (T1D) in senescence-accelerated prone 8 (SAMP8) and senescence-resistant 1 (SAMR1) mice. Contextual fear conditioning demonstrated that T1D resulted in the development of cognitive deficits in SAMR1 mice similar to those seen in age-matched, nondiabetic SAMP8 mice. No further cognitive deficits were observed when the SAMP8 mice were made diabetic. T1D dramatically increased Aβ and glial fibrillary acidic protein immunoreactivity in the hippocampus of SAMP8 mice and to a lesser extent in age-matched SAMR1 mice. Further analysis revealed aggregated Aβ within astrocyte processes surrounding vessels. Western blot analyses from T1D SAMP8 mice showed elevated amyloid precursor protein processing and protein glycation along with increased inflammation. T1D elevated tau phosphorylation in the SAMR1 mice but did not further increase it in the SAMP8 mice where it was already significantly higher. These data suggest that aberrant glucose metabolism potentiates the aging phenotype in old mice and contributes to early stage central nervous system pathology in younger animals.

Key words: advanced glycation end-products; aging; Alzheimer's disease; amyloid angiopathy; diabetes; neurovascular inflammation.

Introduction

Diabetes is a disorder of glucose metabolism characterized by the impaired ability to either produce or respond to insulin, leading to hyperglycemia. It is a chronic disease with severe complications that include renal failure, vision loss, peripheral neuropathy, stroke, and coronary heart disease (Gerich, 1986; Roriz-Filho *et al.*, 2009). Diabetes can also cause complications in the central nervous system (CNS) leading to morphological, electrophysiological, and cognitive changes (Biessels *et al.*, 2008; Roriz-Filho *et al.*, 2009; Wrighten *et al.*, 2009). Many of the CNS changes in diabetic patients resemble those associated with normal aging as well as with vascular dementias and Alzheimer's disease (AD) (Maher & Schubert, 2009; Akter *et al.*, 2011). Indeed, numerous epidemiological studies support a link between diabetes and AD, showing that diabetic patients over 65 years of age have a significantly increased risk of developing AD (For review see Maher & Schubert, 2009). The hippocampus, a brain structure severely affected in AD, is also very sensitive to changes in glucose homeostasis (Wrighten *et al.*, 2009) and is compromised in old age [For review see (Bishop *et al.*, 2010)].

It has been argued that neurovascular dysfunction is central to the development and progression of AD (Deane & Zlokovic, 2007; Grammas, 2011). As the vascular endothelium is particularly affected by hyperglycemia in diabetes (Mazzone *et al.*, 2008) and the blood–brain barrier (BBB) is compromised in a mouse model of type 1 diabetes (T1D) (Huber *et al.*, 2006), dysfunction of the brain vasculature may provide a link between diabetes and AD.

We have recently shown in cultured microvascular endothelial cells that hyperglycemia and beta amyloid peptide (Aβ) synergize to accelerate the production of reactive oxygen species (ROS) and advanced glycation end-products (AGEs) (Burdo *et al.*, 2009). In addition, the induction of T1D with streptozotocin (Stz) in familial AD transgenic mice exaggerated both vascular and AD-linked pathology (Burdo *et al.*, 2009; Jolivalt *et al.*, 2010). Similar results were obtained with APP^{+}-ob/ob type 2 diabetic (T2D) mice, which showed enhanced, AD-like cognitive dysfunction together with cerebrovascular inflammation and amyloid angiopathy (Takeda *et al.*, 2010).

The vast majority of the mouse models used to study the diabetes/AD interaction rely on genetic manipulation to generate models of familial AD, which account for less than 5% of all AD cases (Swerdlow, 2007). However, these models do not reflect the natural onset and progression of the disease that occurs for the most patients. The well-studied senescence-accelerated prone 8 (SAMP8) mice develop early deterioration in learning and memory (6 months) as well as a number of brain alterations similar to those found in AD, including increased oxidative stress, gliosis, Aβ deposition, and tau phosphorylation (Pallas *et al.*, 2008; Takeda, 2009). The SAMP8 mouse is not dominated by the overproduction of Aβ, and therefore serves as a better model to investigate the spontaneous causation of AD, while allowing the investigation of the physiological mechanisms of aging and how diabetes can impact the aged brain. Here, we used the SAMP8 mice along with their corresponding control, the SAMR1 mice, to examine the contributions of diabetes to AD-related pathology in the aged brain. This study focused on both the neurovascular axis and the metabolism of the amyloid precursor protein (APP) because of the central role played by both in diabetes and AD. We reasoned that this approach could provide valuable clues as to the primary pathological mechanisms that underlie the contributions of diabetes to the dysfunction of the aging brain. It is shown here that T1D increases vascular-associated Aβ deposition in the brain and causes accelerated brain aging as compared with nondiabetic animals.

Correspondence
Pamela Maher, Laboratory of Cellular Neurobiology, The Salk Institute for Biological Studies, 10010 N. Torrey Pines Rd. La Jolla, CA 92037, USA.
Tel.: +1 858 453 4100; fax: +1 858 535 9062; e-mail: pmaher@salk.edu

Accepted for publication *23 August 2012*

Aging Cell

Results

Induction of type 1 diabetes

At 6 months of age, SAMP8 mice exhibited reduced weights compared with the control SAMR1 mice but both groups had similar blood glucose levels (Fig. 1A). T1D was induced by the administration of Stz, and blood glucose was monitored regularly in both Stz and Sham groups for a period of 4 months before sacrifice. Although there was a slight drop in the body weights following administration of Stz, this was not statistically significant (Fig. 1B). An increase in blood glucose levels was observed in both sets of Stz-treated mice, which stabilized about forty days later at statistically significant, hyperglycemic levels (Fig. 1C), indicating that the Stz-treated mice developed T1D. One T1D SAMP8 mouse died during the course of this study and was not part of the following analyses. No other fatalities occurred.

Age-related behavioral impairment in diabetic mice

As the progression of diabetes can lead to cognitive dysfunction (Biessels *et al.*, 2008; Roriz-Filho *et al.*, 2009; Wrighten *et al.*, 2009), we carried out a comprehensive behavioral assessment of the mice beginning at nine months of age, testing both locomotor and cognitive parameters. The open field test was used to examine locomotor activity. Although the distance travelled was not statistically different between groups, there was a trend to lower average velocities with T1DM and in SAMP8 mice (Fig. 2A,B) with a statistically significant difference between the T1DM SAMP8 mice and the SAMR1 controls.

The mice were then assayed in multiple memory paradigms including the object recognition and location tests, as well as the Barnes maze. However, we found complications in obtaining valid data with the SAMR1 mice, which appeared to have impaired vision. Indeed, there is a report of accelerated photoreceptor cell degeneration in the SAMR1 mice (Shoji *et al.*, 1998). To circumvent this problem, a fear conditioning test that does not rely on visual capacity was used to measure hippocampal-dependent associative learning. Context-dependent freezing was measured to evaluate the learned aversion of an animal for the environment associated with the mild aversive stimulus. We found that, despite decreased locomotor activity, both the SAMP8 Sham and the T1D SAMR1 mice froze much less than the SAMR1 Sham controls indicating impaired hippocampal function in SAMP8 sham and T1D SAMR1 mice compared with SAMR1 sham mice (Fig. 1C). No further decrease in time freezing was observed in the T1D SAMP8 mice. These results indicate that T1D has detrimental effects on hippocampal-dependent associative learning that is similar to the effect of aging.

Diabetes contributes to Alzheimer's disease-related pathology

We next determined whether or not the behavioral changes seen with aging and diabetes correlated with AD-related pathology in the hippocampus. Alzheimer's disease is characterized by two major pathological features: the aggregation of Aβ into extracellular plaques and the intracellular accumulation of neurofibrillary tangles composed of hyperphosphorylated tau protein. Amyloid precursor protein matures (mAPP) through the constitutive secretory pathway and is then processed by either a nonamyloidogenic or an amyloidogenic route. Amyloidogenic processing involves the formation of the C83 and C99 C-terminal fragments, a consequence of mAPP cleavage by β-secretase, followed by γ-secretase cleavage to generate $A\beta_{1\text{-}40}$ and $A\beta_{1\text{-}42}$, respectively (Thinakaran & Koo, 2008).

(A)

Sham + Stz	Weight (g)	Glucose (mg/dl)
SAMR1	33.2 ± 0.7	174.5 ± 7.7
SAMP8	26.9 ± 1.1 ***	185.4 ± 7.0

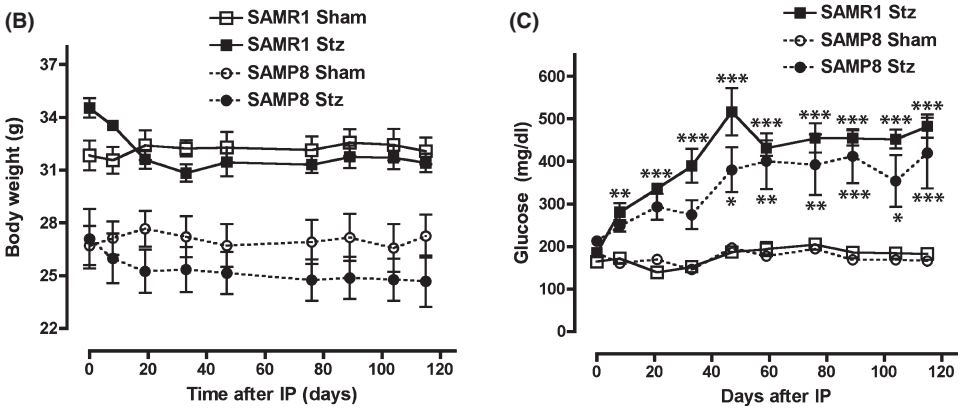

Fig. 1 Induction of type 1 diabetes (T1D) in SAMR1 and SAMP8 mice. Weights and blood glucose levels of 6-month-old T1D (A) SAMR1 and SAMP8 mice were measured at the beginning of the study. SAMP8 mice presented lower weights than SAMR1 mice, but glucose levels were not statistically different. ***$P < 0.001$, *t*-test (n = 8–12/group). To induce T1D, SAMR1, and SAMP8 mice were administered Stz and monitored for four months before sacrifice. Controls (Sham) were given saline injections in parallel. (B) Weights of SAMR1 and SAMP8 Stz mice dropped slightly, but not significantly. (C) Glucose levels increased about threefold in SAMR1 and SAMP8 mice after Stz, and statistically significant hyperglycemia was reached in both groups after forty days. *$P < 0.05$, **$P < 0.01$, ***$P < 0.001$, two-way repeated measures ANOVA and *post hoc* Bonferroni corrected t-test (n = 4–7/group). All data are mean ± SEM.

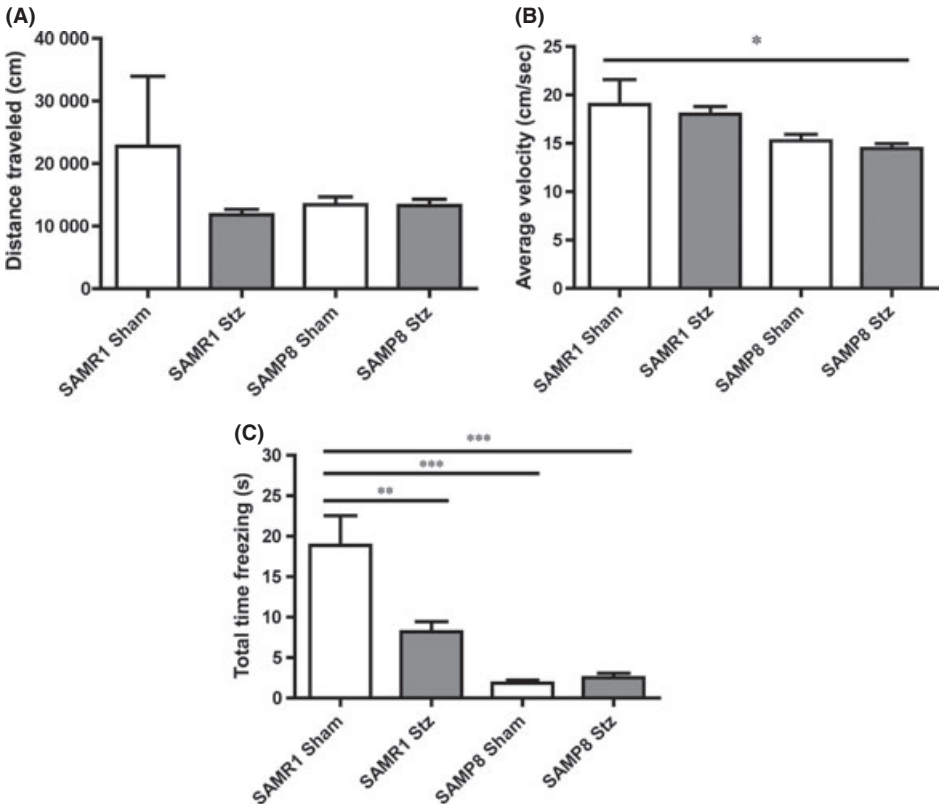

Fig. 2 Behavioral assessment of diabetic SAMR1 and SAMP8 mice. Type 1 diabetes (T1D) mice were assessed for locomotor and cognitive function beginning at nine months, one month prior to sacrifice. Distance traveled (A) and average velocity (B) of T1D mice were assessed in the open field test. There was a trend toward lower activity in the SAMP8 mice with significantly different velocities between the T1D SAMP8 mice and the SAMR1 control mice. (C) The fear conditioning test showed that SAMP8 mice had lower contextual freezing time, suggestive of impaired hippocampal-dependent associative learning. T1D had a similar effect in the SAMR1 mice but did not further exacerbate the decrease in the SAMP8 mice. $*P < 0.05$, $**P < 0.01$, $***P < 0.001$, one-way ANOVA followed by Newman–Keuls *post hoc* test (n = 4–7/group). All data are mean ± SEM.

Although the total levels of APP were not altered under any of the conditions (Fig. 3A,B), there were clear differences in APP maturation and its cleavage products between the various groups (Fig. 3A to E). Both SAMP8 control and T1D SAMP8 mice had higher amounts of mAPP relative to imAPP as compared with SAMR1 mice (Fig. 3A,C), suggestive of increased APP processing. Differences in the levels of C83 and C99 were also seen with the T1D SAMP8 mice showing significant increases when compared with any other group (Fig. 3A,D,E).

As the levels of Aβ in the brains were too low to be detected by Western blotting, we carried out immunohistochemical (IHC) staining that was not only more sensitive but also allowed the localization of Aβ within the hippocampus. There was an increase in Aβ immunoreactivity in the hippocampus of the SAMP8 mice as compared with the SAMR1 mice, and this was further increased by T1D (Fig. 3F,G). Aβ immunoreactivity in the hippocampus was also increased to a lesser extent by T1D in the SAMR1 mice (Fig. 3F,G). The Aβ appeared to be aggregated in vessel-shaped structures in the stratum lacunosum moleculare (SLM), the most highly vascularised region of the hippocampus (Duvernoy, 2005). Confocal microscopy confirmed that most of the Aβ accumulation was indeed surrounding, but not within, brain vessels that were stained with the endothelial marker CD31 (Fig. 4A). Additional confirmation of Aβ accumulation was obtained using specific antibodies to $A\beta_{1\text{-}40}$ and $A\beta_{1\text{-}42}$ which indicated that both forms were detectable in the SLM of the hippocampus of control SAMP8 mice as well as in the hippocampi of T1D SAMR1 and SAMP8 mice (Fig. 4B) but not in the control SAMR1 animals.

With respect to tau pathology, there was an increase in tau phosphorylation at Ser396, an epitope affected in the human AD brain (Ikura *et al.*, 1998), in SAMP8 control mice relative to SAMR1 control mice (Fig. 3H,J). Type 1 diabetes significantly elevated the levels of phospho-tau S396 in the SAMR1 mice but did not further increase them in the SAMP8 mice. No changes in total levels of tau were identified (Fig. 3H,I). These results show that there is perivascular Aβ accumulation that occurs with aging and that is elevated by T1D in young mice and further elevated by T1D in old mice. In contrast, while aging also increases tau phosphorylation, T1D only elevates it in phenotypically younger animals.

Increased astrocytosis is associated with Alzheimer's disease-related pathology in diabetic SAMR1 and SAMP8 mice

Together with vascular endothelial cells, astrocytes are key constituents of the blood–brain barrier (BBB), which has a crucial role in nerve cell maintenance (Abbott *et al.*, 2006). Importantly, astrocytic reactivity is increased in the AD brain in close proximity with amyloid plaques, and Aβ-positive granules have been identified inside astrocytes with a possible implication for Aβ clearance (Mulder *et al.*, 2011). We found an increased expression of glial fibrillary acidic protein (GFAP), an astrocyte marker, in the hippocampus of SAMP8 control mice compared with SAMR1 control mice by Western blotting (Fig. 5A,B). T1D elevated GFAP levels in the SAMR1 mice but did not increase it further in SAMP8 mice (Fig. 5A,B). Immunohistochemical staining confirmed the Western blotting results, demonstrating an increase in the number of astrocytes as well as the

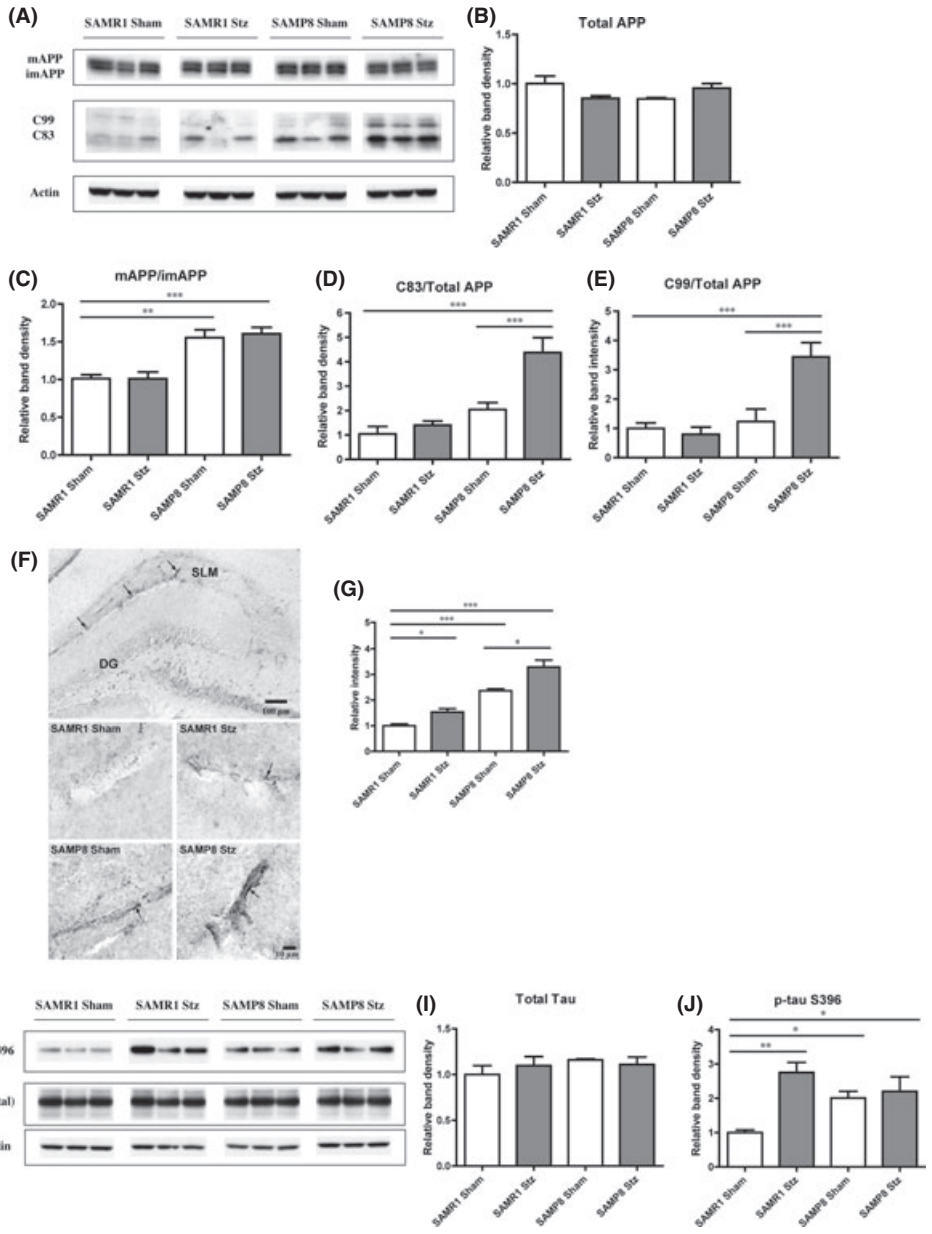

Fig. 3 AD-related pathology in the hippocampus of type 1 diabetes (T1D) mice. T1D SAMR1 and SAMP8 mice were sacrificed four months after administration of Stz, and their brains were removed and processed for both Western blot (WB) and immunohistochemistry (IHC). (A) WB analysis of amyloid precursor protein (APP) processing in RIPA-soluble fraction of hippocampal tissue, using an antibody against the C-terminus of APP. Full-length APP, both its mature (mAPP) and immature (imAPP) forms, and the APP cleavage products C99 and C83 were detected. Actin was used as a loading control. (B) Quantification of the levels of total APP (mAPP + imAPP) in relation to actin. (C) A significant increase in mAPP relative to imAPP in both the SAMP8 Sham and T1D mice was identified, along with elevated levels of C99 (D) and C83 (E) only in the T1D SAMP8 mice. $^{**}P < 0.01$, $^{***}P < 0.001$, one-way ANOVA followed by Newman–Keuls *post hoc* test (n = 5–6/group). (F) IHC analysis of Aβ in the hippocampus identified blood vessel shaped-like reactivity, particularly noticeable in the stratum lacunosum moleculare (SLM). Original magnifications: ×100 (first panel, SAMP8 T1D) and ×630 (rest of the panels). (G) Quantification of Aβ revealed increased reactivity (arrows) in SAMP8 mice. T1D increased Aβ aggregation in both the SAMR1 and the SAMP8 mice. $^{*}P < 0.05$, $^{***}P < 0.001$, one-way ANOVA followed by Newman–Keuls *post hoc* test (n = 3/group). (H) WB analysis of total tau and tau phosphorylated at Ser396 (p-tau S396) in RIPA-soluble fractions of hippocampal tissue. No changes in total tau levels, relative to actin, were identified between the groups (I); however, T1D SAMP8 and Sham mice and T1D SAMR1 mice showed significantly higher levels of p-tau S396 in comparison with the SAMR1 Sham mice (J). $^{*}P < 0.05$, $^{**}P < 0.01$, one-way ANOVA followed by Newman–Keuls *post hoc* test (n = 4–5/group). All data are mean ± SEM.

intensity of GFAP staining, which correlated with morphological changes toward a more ramified shape, indicative of astrocytic reactivity (Fig. 5C,D). Some astrocytes appeared to be associated with blood vessels (Fig. 5C), possibly due to the role that they play as part of the BBB. Glial fibrillary acidic protein immunoreactivity in these structures was higher both in SAMP8 mice and in T1D SAMR1 mice relative to control SAMR1 mice. This staining was very specific to the SLM, the same region where we identified the Aβ aggregates (Fig. 3F). Double staining of GFAP with Aβ in the hippocampus of T1D SAMP8 mice, where the changes were the most dramatic, confirmed that the vessel-shaped GFAP staining was associated with the Aβ aggregates, providing evidence for the localization of the Aβ aggregates inside the astrocytes (Fig. 5E).

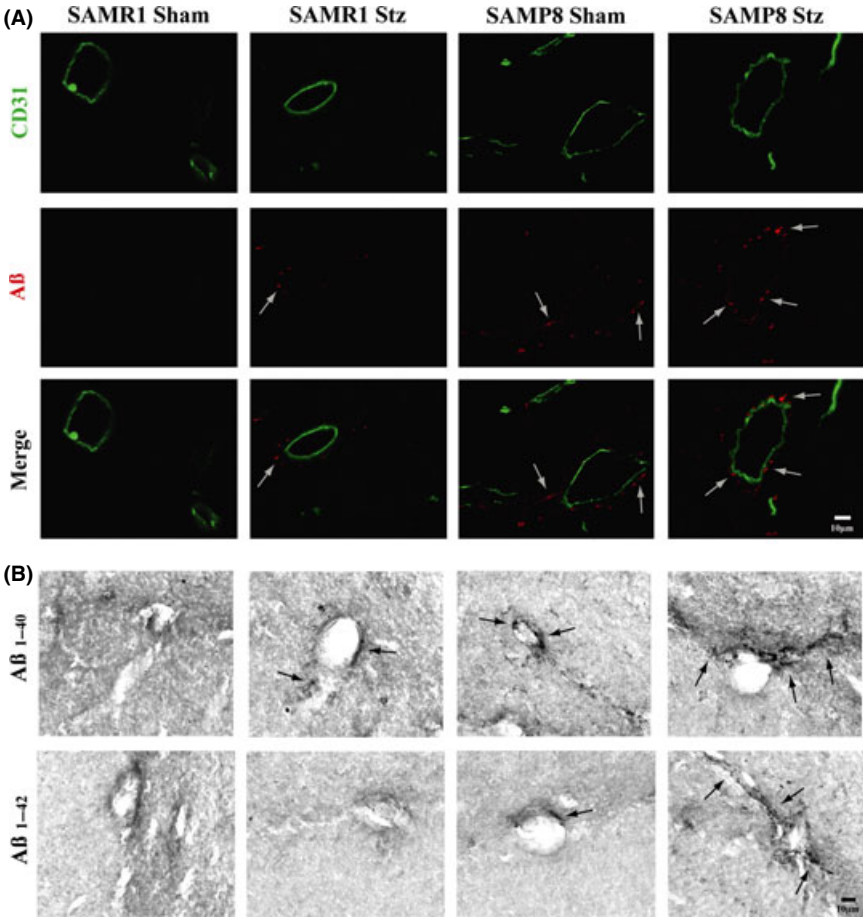

Fig. 4 Immunohistochemical analysis of Aβ distribution. (A) IHC confocal microscopy analysis showed that the Aβ aggregation (arrows) detected in the SLM of the hippocampus was consistently localized around blood vessels stained with CD31. (B) IHC analysis of the specific $A\beta_{1\text{-}40}$ and $A\beta_{1\text{-}42}$ forms visually confirmed a qualitative increase in vascular amyloid aggregation (arrows) in SAMP8 mice and in T1D SAMR1 and SAMP8 mice. Original magnifications: ×630.

Protein glycation and inflammation in diabetic SAMR1 and SAMP8 mice

The accumulation of AGEs is a feature of both aging and diabetes that is elevated in AD (Srikanth *et al.*, 2011). Advanced glycation end-products can activate both inflammatory and oxidative stress pathways (Singh *et al.*, 2001), which have been linked to both aging and cerebrovascular disease (Srikanth *et al.*, 2011). To determine whether the amyloid and astrocytic changes we identified could be related to the production of AGEs, we assayed both carboxymethyl lysine (CML) and methylglyoxal (MG)-derived AGEs in hippocampal tissue. Carboxymethyl lysine -derived AGEs are glycoxidation products, serving as general biomarkers of oxidative stress (Singh *et al.*, 2001). MG is one of the most potent glycating agents, and its production is directly coupled with glycolysis (Thornalley, 1996). We found that SAMP8 mice had higher levels of CML in the proteins of the hippocampus than SAMR1 mice. T1D increased the level of CML-modified proteins in the SAMR1 mice but did not elevate it further in the SAMP8 mice (Fig. 6A,B). In contrast, MG-modified protein levels were only increased in T1D SAMP8 mice (Fig. 6C,D). The levels of glyoxalase 1 (Glo1), the cellular enzyme responsible for the detoxification of MG, were extremely low in the SAMP8 mice as compared with the control SAMR1 mice and were not further reduced by T1D in the SAMP8 mice (Fig. 6E,F). In contrast, T1D reduced Glo1 levels in the SAMR1 mice (Fig. 6E,F). These results suggest that while both T1D and age lead to a decrease in Glo-1 levels, only the combination of age and T1D leads to the enhanced accumulation of MG-modified proteins (Fig. 6C,D).

As glycation activates pro-inflammatory pathways, we measured the levels of the inflammatory marker COX2 and found that COX2 was only significantly elevated in the T1D SAMP8 (Fig. 6G,H). Interestingly, the levels of SOD1, an important cellular antioxidant enzyme, were, like COX2 and MG-dependent protein glycation, only elevated in T1D SAMP8 mice (Fig. 6I,J). The levels of SAP102, a marker of synaptic function, were decreased only in the T1D SAMP8 mice (Fig. 6K,L), showing that there was some degradation of synaptic integrity with the combination of age and T1D. Also, as a measure of synaptic homeostasis, the expression of pro-BDNF, the precursor of BDNF, a neurotrophin essential for synaptic plasticity and cognitive function (Greenberg *et al.*, 2009) was measured. We found that control SAMP8 mice had lower levels than control SAMR1 mice. T1D reduced pro-BDNF levels in the SAMR1 mice but did not cause a further reduction in the SAMP8 mice (Fig. 6M,N).

Discussion

An increasing number of studies support a link between diabetes and AD (for reviews see Maher & Schubert, 2009; Akter *et al.*, 2011), and animal studies, mostly in transgenic mice, demonstrate a diabetes-enhanced progression toward the AD phenotype (Burdo *et al.*, 2009; Jolivalt *et al.*, 2010; Takeda *et al.*, 2010). Although it is widely recognized that aging is

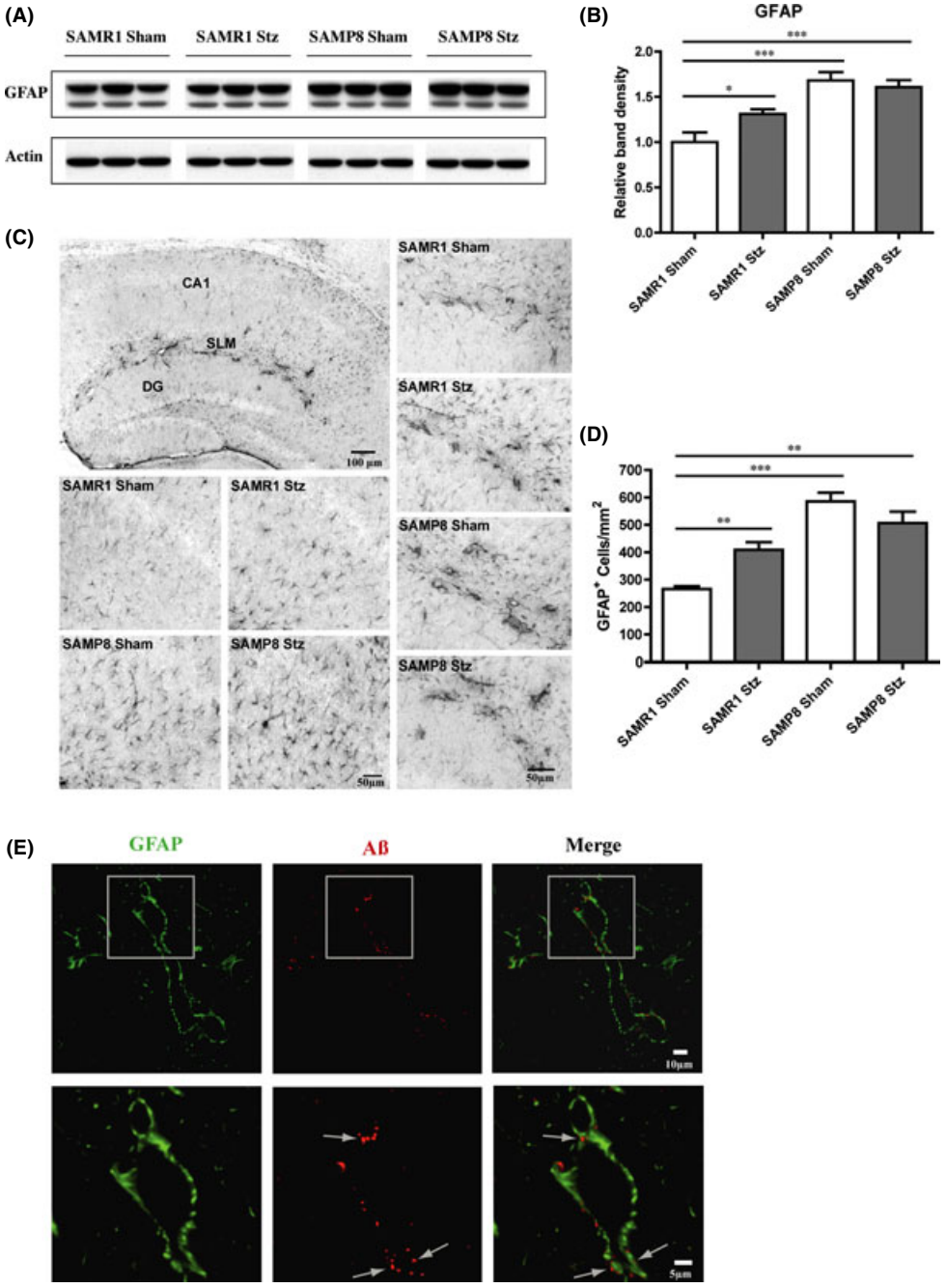

Fig. 5 Astrocytosis in the hippocampus of type 1 diabetes (T1D) mice. (A) WB analysis of GFAP in the RIPA-soluble fraction of hippocampal tissue. (B) Increased GFAP levels (relative to actin) were identified in SAMP8 mice as compared with SAMR1 control mice. Type 1 diabetes also elevated GFAP levels in SAMR1 mice but did not further increase them in SAMP8 mice. $*P < 0.05$, $***P < 0.001$, one-way ANOVA followed by Newman–Keuls *post hoc* test (n = 4–5/group). (C) Immunohistochemical (IHC) analysis of GFAP in the hippocampus confirmed increased numbers of GFAP-positive astrocytes in SAMP8 mice and T1D SAMR1 mice, as quantified in (D), accompanied by morphological changes toward more ramified shapes as can be seen in (C). Increased GFAP expression was particularly noticeable at the SLM, appearing to be associated with blood vessels [(C), first panel, SAMP8 T1D, and right panels]. $**P < 0.01$, $***P < 0.001$, one-way ANOVA followed by Newman–Keuls *post hoc* test (n = 3/group). Original magnification: ×100. All data are mean ± SEM. (E) IHC confocal microscopy analysis shows that the Aβ aggregation (arrows) detected in the SLM of the hippocampus of T1D SAMP8 mice (also verified in the other groups where Aβ aggregation was elevated) was consistently associated with GFAP-positive cells indicating the presence of Aβ within astrocytes. Original magnification: ×630.

the greatest risk factor for AD, this is the first study to investigate the impact of diabetes on brain function in aging, nontransgenic mice. The premature aging SAMP8 mice exhibit an age-related deterioration in learning and memory, and when near death, develop a number of brain alterations similar to those found in AD, including increased oxidative stress, gliosis, Aβ levels, and tau phosphorylation, while the control SAMR1 strain, developed from the same genetic pool of AKR/J mice, have a normal lifespan (Pallas *et al.*, 2008; Takeda, 2009). Using these mice, we have addressed how T1D interacts with age to contribute to AD-related pathology. We show that T1D elicits a wide range of patho-

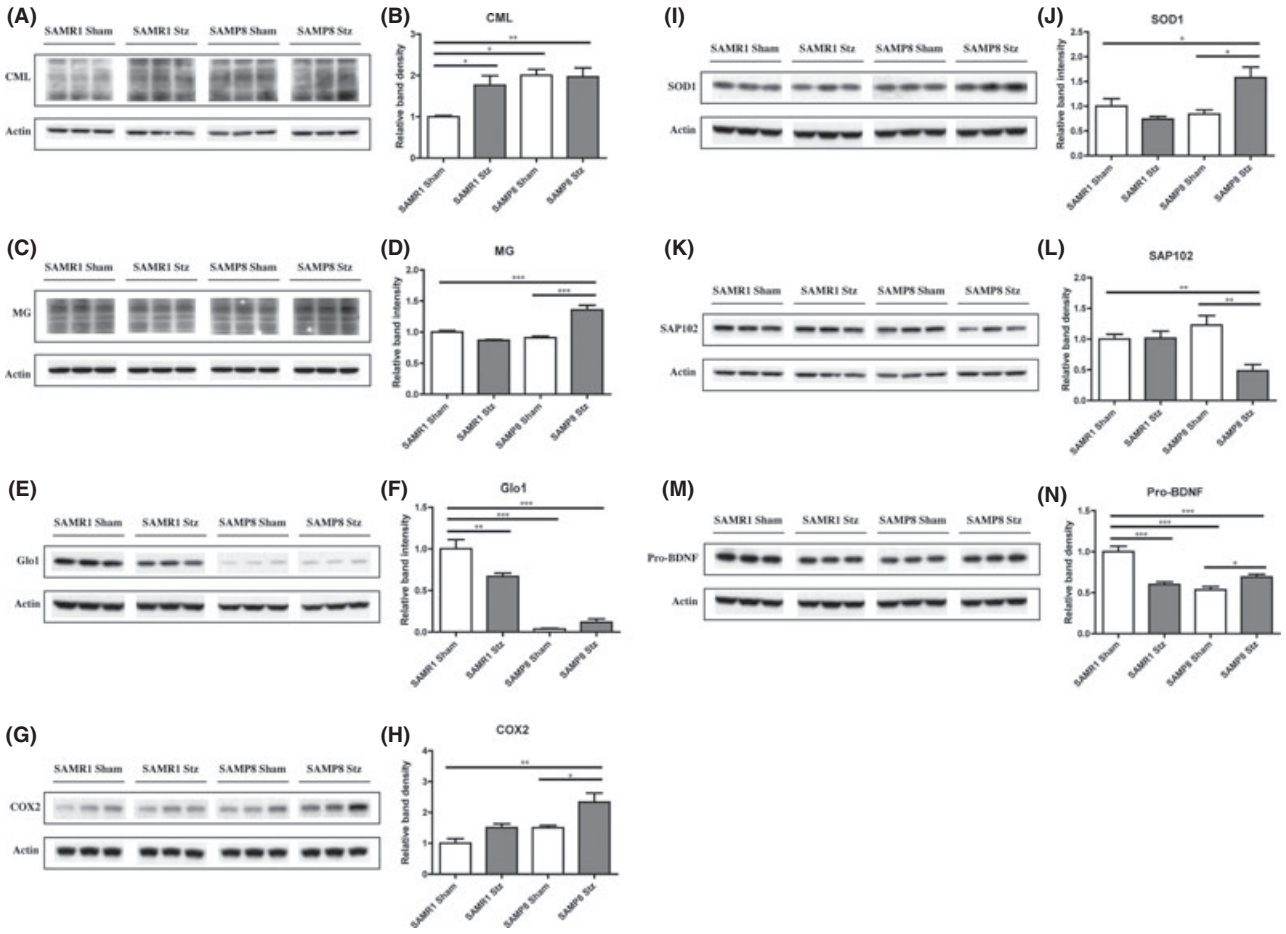

Fig. 6 Hippocampal expression of glycation and inflammation markers in type 1 diabetes (T1D) mice. RIPA-soluble fractions from hippocampal tissue of control and T1D SAMR1 and SAMP8 mice were analyzed by WB for relevant markers of glycation [carboxymethyl lysine (CML) (A) (B); MG (C) (D); Glo1 (E) (F)], inflammation [COX2 (G) (H)], oxidative stress [SOD1 (I) (J)], and neuronal homeostasis [SAP102 (K) (L); Pro-BDNF (M) (N)]. $*P < 0.05$, $**P < 0.01$, $***P < 0.001$, one-way ANOVA followed by Newman–Keuls *post hoc* test (n = 4–5/group). All data are mean ± SEM.

logical changes in the brains of both strains of mice, which are exacerbated by the premature aging phenotype. Namely, T1D induces an AD-related brain pathology in SAMR1 mice, which is in accordance with previous findings in diabetic models (Burdo *et al.*, 2009; Jolivalt *et al.*, 2010; Takeda *et al.*, 2010). However, our study is the first to show that these modifications are similar to those seen in old, nondiabetic SAMP8 mice and to further identify unique pathological changes, such as increases in markers of inflammation and protein glycation, in aged, T1D SAMP8 mice. In addition, we detected severe diabetes-induced amyloid pathology in these mice derived from endogenous, not transgenic Aβ. Finally, we provide valuable clues as to the involvement of the BBB in the pathology, showing that the accumulation of Aβ mostly takes place inside astrocytes associated with the vasculature, which is in accordance with findings from cell culture and human AD studies (Utter *et al.*, 2008) (Mulder *et al.*, 2011), but which, to our knowledge, had not been shown previously in a T1D model.

Behavioral assessment showed that T1D impaired hippocampal-dependent learning in the SAMR1 mice similarly to the aging-accelerated SAMP8 mice. In addition, the molecular and histological data indicate that aging, as represented by the SAMP8 mice, greatly enhances the impact of T1D on hippocampal homeostasis, leading to the development of AD-related pathology. When compared to the SAMR1 mice of the same age, SAMP8 mice have higher levels of Aβ, which were further increased by T1D. Furthermore, the diabetic SAMP8 mice showed a significant increase in the C99 and C83 APP-cleaved products. As the amyloidogenic processing involves the formation of the C83 and C99 C-terminal fragments that are later cleaved to generate Aβ (Thinakaran & Koo, 2008), this could, at least, partially explain the higher levels of Aβ found in the T1D SAMP8 mice. mAPP was elevated in the SAMP8 mice even in the absence of diabetes, and it is possible that an increase in APP maturation predisposes APP to the increased Aβ detected in the T1D SAMP8 mice. Importantly, while diabetes increases amyloid pathology in APP transgenic mice (Burdo *et al.*, 2009; Jolivalt *et al.*, 2010; Takeda *et al.*, 2010), we show here that endogenous mouse Aβ can also accumulate as a result of diabetes.

Aβ accumulation in the hippocampus of SAMP8 mice has been reported (Kumar *et al.*, 2000; Del Valle *et al.*, 2010), with clusters of Aβ found associated with blood vessels (Del Valle *et al.*, 2011). We expand upon these findings and show that Aβ aggregation, which was pronounced in the T1D SAMP8 mice, was consistently associated with reactive astrocytes that wrap around the blood vessels in the SLM of the hippocampus. Astrocytes are the most abundant type of glial cell in the CNS and appear to be involved in both the induction of neuroinflammation (Li *et al.*, 2011) and in the clearance of Aβ (Mulder *et al.*, 2011). In addition, Aβ accumulates inside perivascular astrocytes in the brains of AD patients with vascular pathology (Utter *et al.*, 2008). Our results are in

accordance with reports from humans (Utter *et al.*, 2008) and provide valuable clues on possible mechanisms that may link diabetes and aging to AD, such as the role of perivascular astrocytes in mediating Aβ homeostasis during inflammation.

SAMP8 mice have a very unique pattern of protein glycation and inflammation markers. Increased protein modification by AGEs is characteristic of aging and is associated with many neurodegenerative diseases such as AD (Srikanth *et al.*, 2011). Therefore, mechanisms that prevent AGE formation or involve the detoxification of its precursors are of particular interest in aging research (Srikanth *et al.*, 2011). Levels of Glo1, the enzyme that detoxifies methylglyoxal (MG), decrease with aging (Xue *et al.*, 2011). Although Glo1 is higher in AD patients at very early stages of the disease, its levels decrease with disease progression (Kuhla *et al.*, 2007). In accordance with human aging (Xue *et al.*, 2011), there were very low levels of Glo1 in the SAMP8 mice. Methylglyoxal production is linearly associated with glycolysis, which, in turn, increases with glucose availability (Thornalley, 1996). Insufficient Glo1 activity, as is found in the SAMP8 mice, could predispose the hippocampus to the detrimental impact of hyperglycemia, explaining the high levels of MG-modified proteins that were found only in the T1D SAMP8 mice. MG-modified proteins as well as other AGEs can trigger inflammation (Srikanth *et al.*, 2011) and increase the levels of COX2, a well-studied inflammation marker found elevated in the brains of AD patients (Hoozemans *et al.*, 2008). SOD1, an enzyme with both antioxidant and pro-oxidant properties (Buettner, 2011), was also elevated only in the T1D SAMP8 mice and was associated with the amyloid pathology. In contrast to MG-dependent protein glycation, the CML modification of proteins was increased in both the SAMP8 mice and the T1D SAMR1 mice relative to control SAMR1 mice. This modification is derived primarily from hexoses and has been associated with old age (Dyer *et al.*, 1993; Schleicher *et al.*, 1997), again suggesting that diabetes drives the brain in the direction of accelerated aging.

Tau phosphorylation at S396 was also elevated in the SAMP8 mice as it is in AD patients (Canudas *et al.*, 2005). Interestingly, T1D increased p-tau S396 in the SAMR1 mice but did not induce a further increase in the SAMP8 mice. Indeed, tau hyperphosphorylation was associated with diabetes in numerous studies (Jolivalt *et al.*, 2008, 2010; Kim *et al.*, 2009). Our data on tau phosphorylation correlated with the behavioral data from the fear conditioning test, while Aβ levels did not. Many other observations suggest that tau pathology is more highly reflective of cognitive decline than amyloid pathology (Berg *et al.*, 1998; Giannakopoulos *et al.*, 2009).

In summary, our study supports and extends the links between diabetes, aging, and AD (Maher & Schubert, 2009; Akter *et al.*, 2011). We show that diabetes affects brain function and enhances the development of features that resemble those of aging that may underlie early pathological events in AD. The idea that cerebrovascular inflammation plays a relevant role in the onset and progression of AD is receiving growing support (Grammas, 2011). In this respect, we found that although both diabetes and aging impaired cognitive function, only T1D in the context of old age induced a condition characterized by elevated APP and vascular Aβ pathology associated with increased MG protein glycation and inflammation. Consistent with the known peripheral targets of T1D (Mazzone *et al.*, 2008), a major CNS target appears to be the vasculature (Deane & Zlokovic, 2007; Grammas, 2011). This observation suggests that a further understanding of the role of the brain vasculature in the regulation of neuronal homeostasis will help to shed light on how dysfunction of the BBB may result in neurological diseases such as AD. The AD field needs new therapeutic targets that allow the treatment of the disease in its early stages, and the neurovascular system appears to be an excellent candidate.

Experimental procedures

Mice

The senescence-accelerated mouse prone 8 (SAMP8) line and the respective more normal aging control senescence-accelerated mouse resistant 1 (SAMR1) were acquired from Harlan Laboratories (Blackthorn, UK).

Induction of T1D in SAMP8 and SAMR1 mice was carried out as previously described (Burdo *et al.*, 2009; Jolivalt *et al.*, 2010). Briefly, insulin-deficient diabetes was induced in 6-month-old male mice following an overnight fast by the intraperitoneal (i.p.) injection of streptozotocin (Stz) (Calbiochem, La Jolla, CA, USA) at 100 mg kg^{-1} dissolved in 0.9% sterile saline, on two successive days. Control mice (four SAMR1 and five SAMP8) were given sham injections of saline solution only. Mouse body weights were monitored regularly, and hyperglycemia was confirmed at regular time points using a strip-operated reflectance meter (AlphaTRAK; Abbot Animal Health, North Chicago, IL, USA) in a blood sample obtained by tail prick. Mice were sacrificed four months after administration of Stz. One T1D SAMP8 mouse died during the course of this study and was not included in the analyses.

All the experiments were performed in accordance with the US Public Health Service Guide for Care and Use of Laboratory Animals and protocols approved by the IACUC at the Salk Institute.

Behavioral assessment

Open field assay

The open field test was performed using MED Associates hardware and the Activity Monitor software according to the manufacturer's instructions (MED Associates Inc., St. Albans, VT, USA). The open-field activity monitoring system contains a subject containment environment (chamber), infrared (I⁄R) sources, and sensors. To perform the test, each mouse was placed in the testing chamber and the activity tracked by the Activity Monitor software for 30 min. Scanning was done every 50 ms.

Fear conditioning assay

The protocol consisted of a training phase where the mice were placed in a chamber with a particular context and first allowed to explore for 2 min. An auditory stimulus (2 kHz, 85 dB intensity) was then presented for 30 s immediately followed by a 2 s foot shock (0.7 mA). After 30 s, a second auditory stimulus followed by foot shock was repeated and mice remained in the chamber for an additional 2 min. Twenty-four hours later, the mice were returned to the training chamber for the same length of time as the previous day and allowed to explore for the entire time (5 min) but without the presentation of a tone or a shock. The amount of time spent freezing by the mice during the entire 5 min in the training chamber was recorded and measured by a camera and Freeze software (Med Associates Inc.). A mouse that remembers the chamber context and associates it with the foot shock of the previous day will spend more time freezing and this response is hippocampus dependent. The percentage time spent freezing by each mouse was averaged per group.

Tissue preparation and Western blotting

Mice were anesthetized, perfused with PBS, and their brains removed. Half of the brain was fixed and processed for histology, and the other half was dissected and prepared for Western blot (WB) analysis. Hippocampal tissue samples were homogenized in 10 volumes of RIPA lysis buffer

(50 mM Tris, pH 7.5, 150 mM NaCl, 0.1% sodium dodecyl sulfate and 0.5% deoxycholate, and 1% NP40) containing a cocktail of protease and phosphatase inhibitors (protease inhibitor cocktail complete mini-EDTA free, 1836170, Roche (Indianapolis, IN, USA); phosphatase inhibitor cocktail 2, P5726, Sigma, St. Louis, MO, USA). Samples were sonicated (2 × 10 s) and centrifuged at 100 000 *g* for 60 min at 4 °C.

Protein concentrations in the cell extracts were determined using the BCA protein assay (Pierce, Rockford, IL, USA). Equal amounts of protein were solubilized in 2.5× SDS sample buffer, separated on 12% or 10–20% SDS-polyacrylamide gels (Bio-Rad, Hercules, CA, USA), transferred to Immobilon P (Millipore, Billerica, MA, USA), and immunoblotted with the following antibodies: APP C-Terminal, 1/100 000 (A8717, Sigma); pro-BDNF, 1/1000 (sc-65514; Santa Cruz Biotechnology, Santa Cruz, CA, USA); COX2, 1/500 (610203; BD Transduction Laboratories, San Jose, CA, USA); carboxymethyl lysine (CML), 1/2000 (ab27684; abcam, Cambridge, MA, USA); GFAP, 1/10 000 (AB5804; Chemicon, Temecula, CA, USA); Glo1, 1/1000 (sc-67351, Santa Cruz Biotechnology); methylglyoxal (MG), 1/1000 (STA-011; Cell Biolabs, San Diego, CA, USA); SAP102, 1/500 (AB5170; Millipore, Temecula, CA, USA); SOD1, 1/10 000 (LF-PA0013; Lab Frontier, Seoul, Korea); total tau, 1/10 000 (A0024; Dako Cytomation, Via Real Carpinteria, CA, USA); and p-tau S396, 1/1000 (9632, Cell Signaling Technology, Danvers, MA, USA). Protein levels were normalized to actin levels (1/25 000, 5125, Cell Signaling Technology). After primary antibody incubation, the blots were developed with the respective horseradish peroxidase-conjugated secondary antibody (Bio-Rad). The antibody conjugates were detected using a chemiluminescence kit (Thermo Scientific, Rockford, IL, USA). Films were scanned using a Bio-Rad GS-800 densitometer and the bands quantified with Quantity One Software (Bio-Rad).

Immunohistochemistry

Brains were drop-fixed in 4% paraformaldehyde in 100 mM sodium tetraborate, pH 9.5, for 24 h, cryoprotected for 48 h with 20% sucrose–potassium–PBS (KPBS), and cryostat sectioned into coronal (30 μm) sections.

3,3′-Diaminobenzidine staining

Sections were submerged in 0.3% H_2O_2 for 10 min to eliminate endogenous peroxidase activity and treated with 1% borate to eliminate free paraformaldehyde. Sections were incubated with primary antibody (Aβ biotinylated (SIG-39156), Aβ 40 (SIG-39166) and Aβ 42 (SIG-39169), 1/1000, Covance, CA; GFAP, 1/2000, AB5804, Chemicon) in 0.3% Triton X-100 in KPBS with 5% blocking serum overnight at 4 °C, and with biotinylated rabbit secondary antibody (only necessary for GFAP, Aβ 40, and Aβ 42) in 0.3% Triton X-100 for 1 h at room temperature. After incubation with secondary antibody and ABC reagent (Vector Laboratories, Burlingame, CA, USA), sections were developed using metal-enhanced DAB solution. Sections were mounted on slides, dried, dehydrated, treated with xylene, and covered using dibutyl phthalate xylene. Images were captured on a Zeiss Axio Observer VivaTome microscope, and image analysis on sections was performed using Axiovision software. To quantify amyloid deposition, the intensity per area of the Aβ staining was measured on hippocampal slices from three different mice of each group, using the Image J software (NIH). Two slices per brain were used, and quantification was focused on vessels of the stratum lacunosum moleculare (SLM) area of the hippocampus (at least eight vascular fields in the SLM per slice were quantified). Number of astrocytes was calculated per mm^2 in the CA regions of the hippocampus (one slice per brain) of three different mice from each group.

Fluorescent staining

Sections were incubated with primary antibodies (Aβ biotinylated, 1/1000, SIG-39156, Covance, CA; CD31, 1/500, 557355, BD pharmingen; GFAP, 1/2000, AB5804, Chemicon) in 0.3% Triton X-100 in PBS with 5% blocking serum overnight at 4 °C. After incubation with the respective secondary antibodies (Streptavidin Alexa Fluor 555 conjugate, 1/1000, S32355, Invitrogen (Carlsbad, CA, USA), for β-Amyloid biotinylated; Alexa Fluor 488 goat anti-rabbit, 1/500, A-11008, Invitrogen, for CD31 and GFAP) for 1 h at RT, sections were mounted on slides and covered with FluoroGel (Electron Microscopy Sciences, Hatfield, PA, USA). Images were captured on a Zeiss LSM laser scanning confocal microscope, and image analysis was performed using Zen 2010 software.

Statistical analysis

For comparison between two groups at a single time point, an unpaired *t*-test was performed. When comparing multiple groups, one-way ANOVA followed by Newman–Keuls *post hoc* test was used. For data regarding multiple time points, two-way repeated measures ANOVA and *post hoc* Bonferroni corrected t-tests were applied. GraphPad Prism 4 was used for the statistical analyses. Data are expressed as group mean ± SEM, and significance of difference is indicated as $*P < 0.05$, $**P < 0.01$ and $***P < 0.001$.

Acknowledgments

This work was supported by grants from NIH (AG039736) (CJ), The Fritz. B. Burns Foundation (DS & PM), The Bundy Foundation (DL & MP), the Fundação para a Ciência e a Tecnologia (SFRH/BPD/78160/2011) and the Alzheimer's Association (PM). We are grateful to Richard Dargusch for the valuable help in the husbandry of the SAMR1 and the SAMP8 mice. We also thank Joseph Bertelsen from Covance for advice and contribution with several Aβ antibodies (SIG-39156, SIG-39166, SIG-39169). The authors have no conflict of interest to declare.

Author contributions

AC designed the research, planned the experiments, collected and analyzed the data, and wrote the paper. MP was involved in the scientific discussion, was helpful in the behavioral assessment and confocal imaging, and analyzed the data and edited the manuscript. DL was involved in the scientific discussion, was helpful in preparing IHC staining, and edited the manuscript. CJ was involved in the scientific discussion, was helpful in generating the T1D mouse model, and edited the manuscript. PM and DS designed the research, were involved in the scientific discussion, and wrote the paper.

References

Abbott NJ, Ronnback L, Hansson E (2006) Astrocyte-endothelial interactions at the blood-brain barrier. *Nat. Rev.* **7**, 41–53.

Akter K, Lanza EA, Martin SA, Myronyuk N, Rua M, Raffa RB (2011) Diabetes mellitus and Alzheimer's disease: shared pathology and treatment? *Br. J. Clin. Pharmacol.* **71**, 365–376.

Berg L, McKeel Jr DW, Miller JP, Storandt M, Rubin EH, Morris JC, Baty J, Coats M, Norton J, Goate AM, Price JL, Gearing M, Mirra SS, Saunders AM (1998) Clinicopathologic studies in cognitively healthy aging and Alzheimer's disease: relation of histologic markers to dementia severity, age, sex, and apolipoprotein E genotype. *Arch. Neurol.* **55**, 326–335.

Biessels GJ, Deary IJ, Ryan CM (2008) Cognition and diabetes: a lifespan perspective. *Lancet Neurol.* **7**, 184–190.

Bishop NA, Lu T, Yankner BA (2010) Neural mechanisms of ageing and cognitive decline. *Nature* **464**, 529–535.

Buettner GR (2011) Superoxide dismutase in redox biology: the roles of superoxide and hydrogen peroxide. *Anticancer Agents Med. Chem.* **11**, 341–346.

Burdo JR, Chen Q, Calcutt NA, Schubert D (2009) The pathological interaction between diabetes and presymptomatic Alzheimer's disease. *Neurobiol. Aging* **30**, 1910–1917.

Canudas AM, Gutierrez-Cuesta J, Rodriguez MI, Acuna-Castroviejo D, Sureda FX, Camins A, Pallas M (2005) Hyperphosphorylation of microtubule-associated protein tau in senescence-accelerated mouse (SAM). *Mech. Ageing Dev.* **126**, 1300–1304.

Deane R, Zlokovic BV (2007) Role of the blood-brain barrier in the pathogenesis of Alzheimer's disease. *Curr. Alzheimer Res.* **4**, 191–197.

Del Valle J, Duran-Vilaregut J, Manich G, Casadesus G, Smith MA, Camins A, Pallas M, Pelegri C, Vilaplana J (2010) Early amyloid accumulation in the hippocampus of SAMP8 mice. *J. Alzheimers Dis.* **19**, 1303–1315.

Del Valle J, Duran-Vilaregut J, Manich G, Pallas M, Camins A, Vilaplana J, Pelegri C (2011) Cerebral amyloid angiopathy, blood-brain barrier disruption and amyloid accumulation in SAMP8 mice. *Neurodegener. Dis.* **8**, 421–429.

Duvernoy HM (2005). *The Human Hippocampus: Functional Anatomy, Vascularization and Serial Sections with MRI*, 3rd edn. New York: Springer.

Dyer DG, Dunn JA, Thorpe SR, Bailie KE, Lyons TJ, McCance DR, Baynes JW (1993) Accumulation of Maillard reaction products in skin collagen in diabetes and aging. *J. Clin. Invest.* **91**, 2463–2469.

Gerich JE (1986) Insulin-dependent diabetes mellitus: pathophysiology. *Mayo Clin. Proc.* **61**, 787–791.

Giannakopoulos P, Kovari E, Gold G, von Gunten A, Hof PR, Bouras C (2009) Pathological substrates of cognitive decline in Alzheimer's disease. *Front Neurol. Neurosci.* **24**, 20–29.

Grammas P (2011) Neurovascular dysfunction, inflammation and endothelial activation: implications for the pathogenesis of Alzheimer's disease. *J. Neuroinflammation* **8**, 26.

Greenberg ME, Xu B, Lu B, Hempstead BL (2009) New insights in the biology of BDNF synthesis and release: implications in CNS function. *J. Neurosci.* **29**, 12764–12767.

Hoozemans JJ, Rozemuller JM, van Haastert ES, Veerhuis R, Eikelenboom P (2008) Cyclooxygenase-1 and -2 in the different stages of Alzheimer's disease pathology. *Curr. Pharm. Des.* **14**, 1419–1427.

Huber JD, VanGilder RL, Houser KA (2006) Streptozotocin-induced diabetes progressively increases blood-brain barrier permeability in specific brain regions in rats. *Am. J. Physiol. Heart Circ. Physiol.* **291**, H2660–H2668.

Ikura Y, Kudo T, Tanaka T, Tanii H, Grundke-Iqbal I, Iqbal K, Takeda M (1998) Levels of tau phosphorylation at different sites in Alzheimer disease brain. *NeuroReport* **9**, 2375–2379.

Jolivalt CG, Lee CA, Beiswenger KK, Smith JL, Orlov M, Torrance MA, Masliah E (2008) Defective insulin signaling pathway and increased glycogen synthase kinase-3 activity in the brain of diabetic mice: parallels with Alzheimer's disease and correction by insulin. *J. Neurosci. Res.* **86**, 3265–3274.

Jolivalt CG, Hurford R, Lee CA, Dumaop W, Rockenstein E, Masliah E (2010) Type 1 diabetes exaggerates features of Alzheimer's disease in APP transgenic mice. *Exp. Neurol.* **223**, 422–431.

Kim B, Backus C, Oh S, Hayes JM, Feldman EL (2009) Increased tau phosphorylation and cleavage in mouse models of type 1 and type 2 diabetes. *Endocrinology* **150**, 5294–5301.

Kuhla B, Boeck K, Schmidt A, Ogunlade V, Arendt T, Munch G, Luth HJ (2007) Age- and stage-dependent glyoxalase I expression and its activity in normal and Alzheimer's disease brains. *Neurobiol. Aging* **28**, 29–41.

Kumar VB, Farr SA, Flood JF, Kamlesh V, Franko M, Banks WA, Morley JE (2000) Site-directed antisense oligonucleotide decreases the expression of amyloid precursor protein and reverses deficits in learning and memory in aged SAMP8 mice. *Peptides* **21**, 1769–1775.

Li C, Zhao R, Gao K, Wei Z, Yin MY, Lau LT, Chui D, Hoi Yu AC (2011) Astrocytes: implications for neuroinflammatory pathogenesis of Alzheimer's disease. *Curr. Alzheimer Res.* **8**, 67–80.

Maher PA, Schubert DR (2009) Metabolic links between diabetes and Alzheimer's disease. *Expert Rev. Neurother.* **9**, 617–630.

Mazzone T, Chait A, Plutzky J (2008) Cardiovascular disease risk in type 2 diabetes mellitus: insights from mechanistic studies. *Lancet* **371**, 1800–1809.

Mulder SD, Veerhuis R, Blankenstein MA, Nielsen HM (2011) The effect of amyloid associated proteins on the expression of genes involved in amyloid-beta clearance by adult human astrocytes. *Exp. Neurol.* **233**, 373–379.

Pallas M, Camins A, Smith MA, Perry G, Lee HG, Casadesus G (2008) From aging to Alzheimer's disease: unveiling ''the switch'' with the senescence-accelerated mouse model (SAMP8). *J. Alzheimers Dis.* **15**, 615–624.

Roriz-Filho JS, Sa-Roriz TM, Rosset I, Camozzato AL, Santos AC, Chaves ML, Moriguti JC, Roriz-Cruz M (2009) (Pre)diabetes, brain aging, and cognition. *Biochim. Biophys. Acta* **1792**, 432–443.

Schleicher ED, Wagner E, Nerlich AG (1997) Increased accumulation of the glycoxidation product N(epsilon)-(carboxymethyl)lysine in human tissues in diabetes and aging. *J. Clin. Invest.* **99**, 457–468.

Shoji M, Okada M, Ohta A, Higuchi K, Hosokawa M, Honda Y (1998) A morphological and morphometrical study of the retina in aging SAM mice. *Ophthalmic Res.* **30**, 172–179.

Singh R, Barden A, Mori T, Beilin L (2001) Advanced glycation end-products: a review. *Diabetologia* **44**, 129–146.

Srikanth V, Maczurek A, Phan T, Steele M, Westcott B, Juskiw D, Munch G (2011) Advanced glycation endproducts and their receptor RAGE in Alzheimer's disease. *Neurobiol. Aging* **32**, 763–777.

Swerdlow RH (2007) Is aging part of Alzheimer's disease, or is Alzheimer's disease part of aging? *Neurobiol. Aging* **28**, 1465–1480.

Takeda T (2009) Senescence-accelerated mouse (SAM) with special references to neurodegeneration models, SAMP8 and SAMP10 mice. *Neurochem. Res.* **34**, 639–659.

Takeda S, Sato N, Uchio-Yamada K, Sawada K, Kunieda T, Takeuchi D, Kurinami H, Shinohara M, Rakugi H, Morishita R (2010) Diabetes-accelerated memory dysfunction via cerebrovascular inflammation and Abeta deposition in an Alzheimer mouse model with diabetes. *Proc. Natl Acad. Sci. U.S.A.* **107**, 7036–7041.

Thinakaran G, Koo EH (2008) Amyloid precursor protein trafficking, processing, and function. *J. Biol. Chem.* **283**, 29615–29619.

Thornalley PJ (1996) Pharmacology of methylglyoxal: formation, modification of proteins and nucleic acids, and enzymatic detoxification – a role in pathogenesis and antiproliferative chemotherapy. *Gen. Pharmacol.* **27**, 565–573.

Utter S, Tamboli IY, Walter J, Upadhaya AR, Birkenmeier G, Pietrzik CU, Ghebremedhin E, Thal DR (2008) Cerebral small vessel disease-induced apolipoprotein E leakage is associated with Alzheimer disease and the accumulation of amyloid beta-protein in perivascular astrocytes. *J. Neuropathol. Exp. Neurol.* **67**, 842–856.

Wrighten SA, Piroli GG, Grillo CA, Reagan LP (2009) A look inside the diabetic brain: contributors to diabetes-induced brain aging. *Biochim. Biophys. Acta* **1792**, 444–453.

Xue M, Rabbani N, Thornalley PJ (2011) Glyoxalase in ageing. *Semin. Cell Dev. Biol.* **22**, 293–301.